

Power ICs: New Cu Frontside processes on 300mm

PVD Manager Technology Development *Mohamed Elghazzali* tells us why Evatec's CLUSTERLINE® 300 is the ideal platform to satisfy the growing demand for 300mm processing and how Evatec process know-how is delivering high performance thick copper layers.

Why copper technology

Silicon-based devices need to improve to stay competitive from a cost and performance perspective. To achieve this, silicon power device production is moving from 200mm to 300mm wafer size and aluminum contact technology is being substituted by copper. In comparison to aluminum, copper provides higher electrical conductivity which results in lower losses and a lower Rds-on (Drain – source on-resistance). Most importantly copper is the technology of choice for Si CMOS today: A power device in copper is compatible with the front end of line processes, enabling direct integration in complex IC packages, e.g. BCD, Power IC.

Aluminum based devices are assembled by solder contact, limiting the flexibility for integration. Complex devices with higher integration require advanced packaging solutions, e.g. flip chip bumping. Advanced packaging solutions based on copper technology are the enabling solution for higher integration density (system in package, embedded dies etc.) and increased energy efficiency.

CLUSTERLINE® 300 – A platform built for front side processes

CLUSTERLINE® 300 is designed for the contamination-free processes and the low particle levels required for front side processes on 300mm. For typical Tungsten-Titanium-Alloy and thick copper single layer processes customers can expect WiW thickness / resistivity uniformities (max,min) <5% (1 Sigma <2.5%) across a 300mm wafer with edge exclusion of 3mm.

CLUSTERLINE® 300 can be configured with up to 6 process modules for degas, deposition or etch. Up to 3 load ports / FOUPS deliver wafers to the Atmospheric Frontend Module (AFEM) equipped with robot and aligner with additional options for integration of wafer buffer stations and additional Interface modules (e.g. high pressure cool). Evatec's highly efficient atmospheric batch degas (ABD) technology developed for the highest throughput Fanout and WLCSP processes is also just one of the additional capabilities that can be added for custom applications.

PVD Technology for WTi/Ti-Cu Processes

Evatec's proprietary PVD module technology is at the heart of the tool. The module enables flexibility in process geometry with target substrate distances in the range of 50 to 80mm. Hardware features focused on maintaining stable process pressures and uniform gas distribution combined with low arcing deliver the process stability and repeatabilities required for high volume production. The limited thermal budget of the substrates necessitates strict control of temperature throughout the entire 5 to 10 μm film deposition process. The principal characteristics of the recently developed cold ESC system ensure that the temperature of the wafer remains below 150°C. This has the beneficial effect of reducing the wafer bow to below 350 μm at a film stress of approximately 180 MPa. In conjunction with the specially designed cathode, this results in the ability to manage high power processes, enhancing overall productivity and providing a reliable processes with minimal in-film particle performance.

Film parameter	Performance
Thickness	5... 10 μm
Deposition rate	>25 nm/s
WiW thickness uniformity	<5% (Max/min)
WiW RS uniformity	<5% (Max/min) (@ 500nm thickness)
WtW thickness uniformity	<2% (Max/min)
WtW RS uniformity	<2% (Max/min) (@ 500nm thickness)
Specific resistivity	2 \pm 0.3 uOhms*cm
Average film stress	app. 180 MPa
Max. wafer bow @5 μm @10 μm	app. 280 μm app. 560 μm
Max. wafer temp @5 μm @10 μm	<100°C <130°C
Mech. particles >0.16 μm	< 10 adders
In-film particles >0.20 μm	< 30 adders

Figure 1: Typical WTi process performance data

“Enjoy lower losses and drain source resistance with copper technology”

Lets take a look at the results

Evatec process know-how optimizes the overall process. Cathode and new developed Cold ESC chuck technologies are designed to enable maximum deposition rates for the highest throughput whilst still maintaining low substrate temperatures. Deposition conditions for both barrier and copper layers are tailored to manage overall film stack stress.

■ WTi deposition

Film performance data of typical WTi films in the range 50 to 200nm deposited using Evatec's PVD cathode technology is shown in Figure 1. Processes can be wide ranged tailored for either compressive or tensile film stress according to customer preference.

■ Thick Copper Layer Deposition

Layer performance for copper films typically in the range 5 to 10 microns is illustrated below in Figure 2. Films typically display low levels of tensile stress.

Particles and process repeatability performance

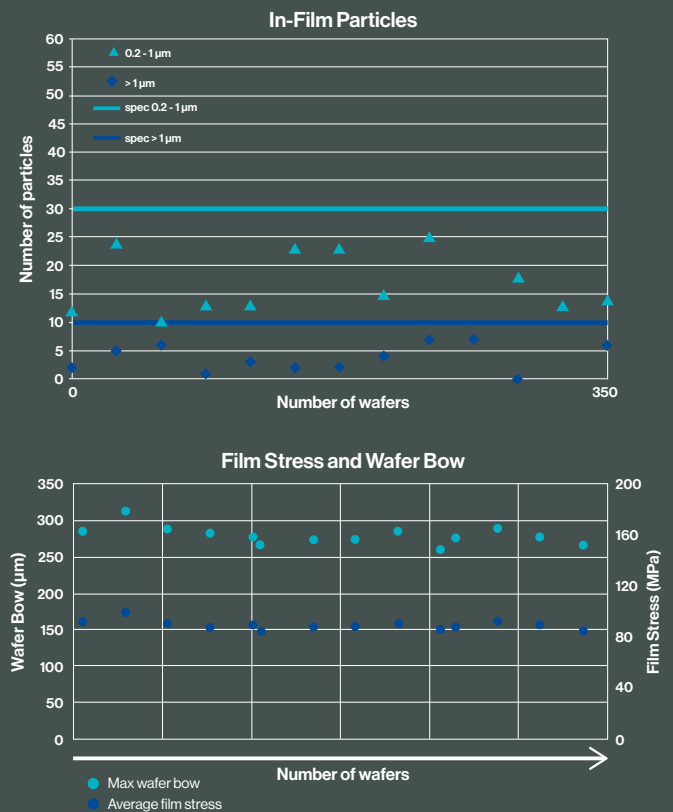


Figure 2: Thick copper deposition process stability

Low-field transport properties and scattering mechanisms of degenerate n-GaN by sputtering from a liquid Ga-target

Dr. Philipp Doering, from Fraunhofer Institute for Applied Solid State Physics (IAF) & *Thomas Tschirky*, Evatec Senior Scientist talk about the work being done on sputtering from a liquid Ga-target.

Abstract

In this work, degenerate n-type GaN thin films prepared by co-sputtering from a liquid Ga-target were demonstrated and their low field scattering mechanisms described. Extremely high donor concentrations above $3 \times 10^{20} \text{ cm}^{-3}$ at low process temperatures ($< 800 \text{ }^\circ\text{C}$) with specific resistivities below $0.5 \text{ m}\Omega\text{cm}$ were achieved. The degenerate nature of the sputtered films was verified via temperature-dependent Hall-measurements (300-550 K) revealing negligible change in electron mobility and donor concentration. Scattering at ionized impurities was determined to be the major limiting factor with a minor contribution of polar optical-phonon scattering at high temperatures. Scattering at dislocations or grain boundaries was ruled out to impact the measured mobility. The results demonstrate the huge potential of sputtering as an alternative route for the realization of low-temperature, high throughput and large-scale, regrown n-type GaN.

The use of GaN-based low-noise and high-power amplifiers as well as their advanced hetero-integration into conventional Si-CMOS technology are of major interest for next generation wireless communication systems. To meet the increased data rate requirements, higher frequencies with improved efficiency and bandwidth are targeted. However, further downscaling of the gate-length (L_g) to address higher cutoff frequencies requires significant reduction of parasitic resistances in the devices.

The access resistance of highly-scaled high-electron mobility transistors (HEMTs) or multi-channel devices suffer from the inherent metal-semiconductor barrier for high Al-content barriers. A current transport mechanism completely determined by tunneling is desirable to achieve the lowest possible voltage drop at the metal-semiconductor interface. Removing the AlGaN-barrier and/or rendering the sub-contact area n-type is the only possibility to change the electron transport across the barrier to the 2-dimension

View of the liquid Ga target through the wafer holder in the prototype sputter module



Sample	Substrate	$t_{n\text{-GaN}}$	T_H	GR	rms	FWHM (00.2)
A	GaN/Sapphire	150 nm	700°C	0.9 nm/s	0.58 nm	0.188°
B	GaN/Sapphire	150 nm	590°C	0.9 nm/s	0.38 nm	–
C	GaN/Sapphire	150 nm	800°C	0.9 nm/s	0.91 nm	0.134°
D	Sapphire	1050 nm	800°C	0.6 nm/s	21.6 nm	0.437°

Table 1: Structural properties of co-sputtered n-GaN: $t_{n\text{-GaN}}$ – thickness of Si-doped GaN-layer, T_H – nom. Heater temperature, GR – growth rate, rms – root mean square, FWHM – full-width half maximum of the 00.2.

electron gas (2DEG) from a thermionic to field-emission type at higher Al-contents. However, to achieve the high doping concentrations ($N_D > 1 \times 10^{20} \text{ cm}^{-3}$) for a completely field emission based current transport is difficult due to the decreasing crystal quality. In addition, low temperature processes on a large wafer scale are beneficial to protect the AlGaIn/GaN-interface in a HEMT or for a direct III-Nitride hetero-integration of (opto-)electronic devices on a Si-based platform.

In this work, the transport properties of heavily Si-doped GaN thin films deposited by co-sputtering from Si and a liquid Ga-target and on 4-inch sapphire substrates are investigated. Extremely high effective donor concentration ($N_D > 3 \times 10^{20} \text{ cm}^{-3}$) are demonstrated. Specific resistivity below 0.5 and 3.5 mΩcm are achieved at growth temperatures of 800°C and 590°C, respectively. Carrier mobilities were found to be limited by scattering at ionized impurities at the high Si doping levels. Donor-acceptor compensation ratio was found nearly constant below $\theta \approx 0.2$ even beyond $N_D > 1 \times 10^{20} \text{ cm}^{-3}$ different to reported data by metalorganic chemical vapor deposition (MOCVD) and molecular beam epitaxy (MBE). Temperature-dependent Hall-measurements revealed negligible change in carrier density and mobility with increasing temperature indicating Mott-transition from a semiconducting to a metallic character. Carrier densities and specific resistivity at low growth temperatures ($\leq 800^\circ\text{C}$) are found well beyond reported data of MOCVD-grown thin films. The results demonstrate the feasibility of sputtered GaN from a liquid Ga-target as alternative process with high carrier density and easy upscaling beyond 4-inch suitable for future process integration into future radio-frequency or optoelectronic (e.g., tunnel junctions) GaN-based devices.

Recent focus on the development of advanced contact processes is generally driven by CMOS-compatible, Au-free and/or low temperature budget ohmic contacts, or n-GaN regrowth for highly-scaled AlGaIn or novel Al(Sc)N-based HEMTs with high Al-content. The fabrication of highly n-type doped GaN films was demonstrated via Si-implantation, MBE, MOCVD (Si or Ge), pulsed laser deposition (PLD) and reactive, pulsed sputtering (PVD) from a solid Ga-target (Si, Ge, Sn, O). Si-implantation is used for GaN-devices but faces issues to achieve carrier densities above $1 \times 10^{19} \text{ cm}^{-3}$ and requires a high-temperature treatment to recover for the implantation damage. MBE-regrown ohmic contact layers are currently the method of choice due to the low growth temperature but faces issue in terms of upscaling, throughput and homogeneity. MOCVD regrowth was demonstrated via flow-modulation epitaxy

at low growth temperatures with reduced growth rate, but faces limitations in terms of achievable carrier density beyond $5 \times 10^{19} \text{ cm}^{-2}$ at 550 °C and does not offer a non-selective growth mode to avoid growth rate inhomogeneities. Typical growth temperatures with high growth rates are conducted at much higher temperatures ($> 950^\circ\text{C}$). Reactive sputtering was demonstrated with high carrier density and high mobility on 300 – 600 nm thick films. However, the used solid Ga-targets need to be heavily cooled to remain solid during sputtering. In addition, the cooling system gets more complex for larger wafer diameters and impurity concentration in e.g., ceramic Ga is not easy to handle. The use of a liquid Ga-target avoids the need of a complex cooling-system required to keep solid Ga-targets below its melting point. The liquid target can be easily filled up and no sputter craters occur during growth. In addition, the liquid target can be easily upscaled to larger wafer diameters ($> 2\text{-inch}$) as well as lower unintentional/parasitic doping occurs when compared to a ceramic Ga-target.

4-inch sapphire substrates were used for the deposition of the conductive thin films. Three samples (A–C) were initially grown by metal-organic chemical vapor deposition with an Fe-doped buffer to render the GaN-layers semi-insulating topped with a 200 nm unintentionally-doped GaN layer to compensate for Fe-segregation. The sheet resistance of samples A, B and C were measured after MOCVD buffer growth via contactless Eddy-current revealing a $R_s > 100 \text{ k}\Omega/\text{sq}$, which is the upper measurement limit of the setup. GaN films were deposited by co-sputtering of a Si-bar and a liquid Ga-target in an Evatec CLUSTERLINE® 200II with a modified process module. 150 nm Si-doped GaN were sputtered on top of the MOCVD-GaN with nominal growth temperature of 590, 700 and 800 °C. Sample D was prepared by directly sputtering GaN:Si on Sapphire. Rocking curves of the 00.2-reflex were carried out by X-ray diffraction to determine the full-width half maxima (FWHM). FWHM were derived from fitting of two pseudo-Voigt functions assuming that the peak with lower intensity is related to the sputtered, Si-doped GaN. The FWHM of the MOCVD-grown buffer was found to be FWHM = 0.064°. Fitting of the sample with lowest growth temperature was not possible due to the low intensity of the second peak. However, it can be concluded that lowering the heater temperature leads to a slight decrease in crystal quality.

Atomic force microscopy (AFM) was used to determine the root mean square (rms) to revealing smoothest surface morphology with lowest growth temperature. A summary of the structural properties is given in Table 1.

The theoretical metal-semiconductor transport properties (thermionic emission - TE, thermionic field emission - TFE; field emission - FE) are dependent on the characteristic energy E_{00} , which in turn is dependent on the carrier density in the sub-contact area as following:

$$E_{00} = \frac{qh}{4\pi} \sqrt{\frac{N_D}{\epsilon_r \left(\frac{m_{tun}^*}{m}\right)}}$$

With q , h , ϵ_r (9.5), m_{tun}^* and m ($m_{tun}^*/m = 0.22$) are the elementary charge, Plancks constant, relative dielectric constant, effective tunneling mass, and electron mass, respectively. We use the simple differentiation: FE: $E_{00} \leq 0.5$ kT; TFE: 0.5 kT $\leq E_{00} \leq 5$ kT and $E_{00} \geq 5$ kT. Thus, to achieve $E_{00} \geq 5$ kT a donor concentration of $N_D > 1 \times 10^{20}$ cm⁻³ is required for GaN. Fundamental low-field transport properties are characterized by Hall-measurements at room-temperature (RT). Ti-based ohmic contacts were evaporated via shadow masks and 4-terminal structures mechanically isolated. The use of a co-sputtering of a Si-bar comes along with the possibility to achieve a gradient in Si-concentration over the same wafer depending on the distance of the wafer area to the Si-bar. Thus, several carrier concentrations and corresponding carrier mobilities can be measured on the same wafer. Carrier densities of $N_D = 6.7 \times 10^{19}$ to 3.7×10^{20} cm⁻³ with carrier mobilities of $\mu = 21$ to 42 cm²/Vs were found over all samples. Improved compensation ratios were found with increasing heater temperature as given in Figure 1. The achieved carrier densities are well beyond the state of the art reported for MOCVD ($N_D < 2.2 \times 10^{20}$ cm⁻³) and MBE ($N_D < 2 \times 10^{20}$ cm⁻³) at generally lower growth temperature (Figure 1c). The achieved carrier densities are exceeding the the $E_{00} \geq 5$ kT = $N_D >$

1×10^{20} cm⁻³ requirement described before. In addition, the extremely high carrier concentrations would be well suited e.g., to address source starvation issues causing linearity distortion in highly scaled GaN-HEMTs.

In general, several scattering mechanisms could be assumed for the co-sputtered GaN:Si even though impurity scattering is most likely dominating at high donor concentrations. Scattering at ionized impurities in dependence of the compensation ratio $\theta = N_D/N_A$ can be expressed by:

$$\mu_{II} = 3(\epsilon_0 \epsilon_r)^2 \left(\frac{h}{q}\right)^3 \left(\frac{n}{N_I}\right) \left(\frac{1}{m_F^*}\right) \left(\ln(1 + \beta_F^2) - \frac{\beta_F^2}{1 + \beta_F^2}\right)^{-1}$$

With:

$$\beta_F^2 = \frac{16m_e^* \epsilon_0 \epsilon_r E_F^2}{3q^2 h^2 n}$$

And N_I and m_F^* are the ionized impurity concentration and effective mass at the Fermi energy, which is given by:

$$m_F^* = m_e^* \left(1 + \frac{6\alpha E_F}{E_g}\right)$$

with

$$E_F = E_F^0 \left(1 + \frac{\alpha E_F^0}{E_g}\right)$$

and:

$$E_F^0 = \left(\frac{h^2 (3\pi^2 n)^{2/3}}{2m_e^*}\right)$$

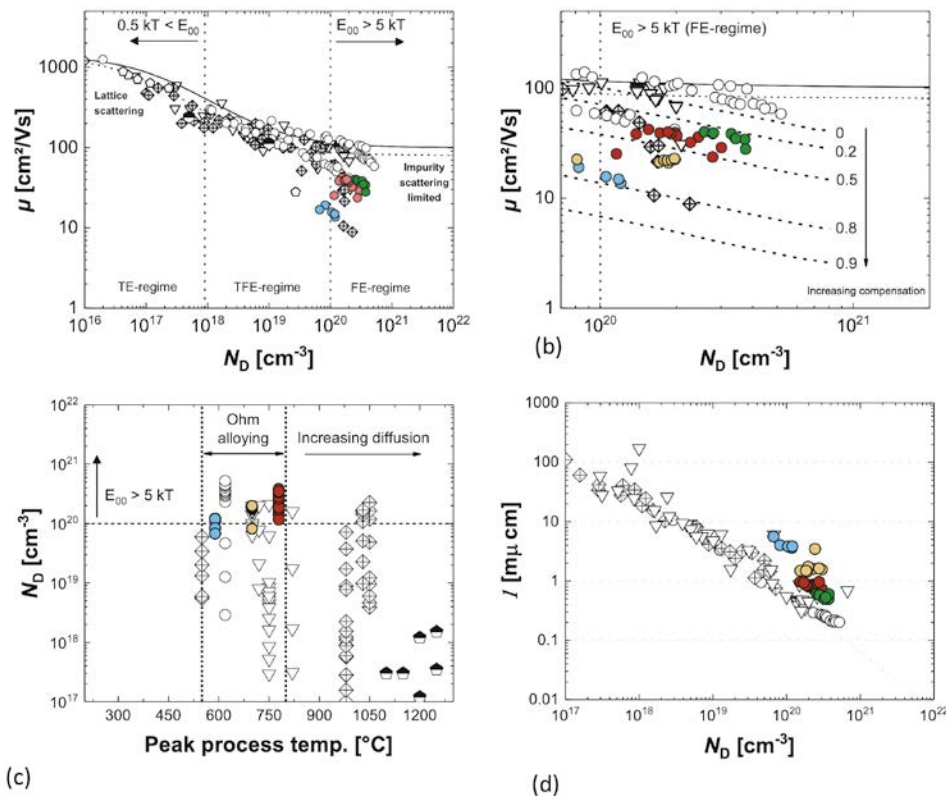


Figure 1: (a) Donor concentration vs. carrier mobility reported in literature for various growth methods: metalorganic chemical vapor deposition (quarters with cross); molecular beam epitaxy (diamonds); hydride vapor phase epitaxy (pentagons) reactive sputtering (grey circles); Si-implantation (half-filled hexagons). Samples in this work are colored: sample A (yellow); B (blue); C (red); D (green). Solid and dotted lines represent fitting from Schwierz et al. based on Caughey-Thomas approximation; (b) N_D vs. μ in the range of $E_{00} > 5$ kT. (c) Peak process temperature vs. measured donor concentration. Reported range of alloying temperatures of ohmic contacts to AlGaIn/GaN are added as a reference; (d) carrier concentration vs. specific resistivity.

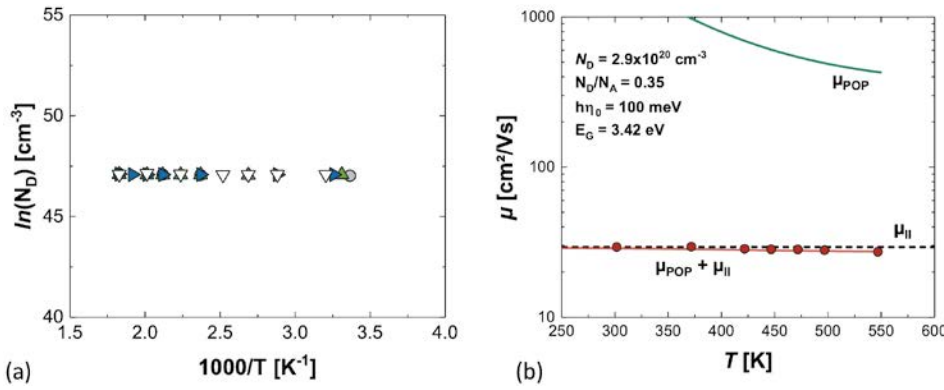


Figure 2: (a) Arrhenius plot of three different positions of sample C; (b) Temperature dependent electron mobility of the heavily doped GaN. Scattering by ionized impurities μ_{ii} (black) and polar optical-phonons μ (green) was modelled to fit the experimental data (red).

Where α (0.64) and m_e^* ($0.22m_e$) are the non-parabolic conduction band coefficient ($\alpha = 1(m_e^*/m_e)^2$), and the electron effective mass, respectively. High carrier compensation ratios $\theta = N_D/N_A$ were found for MOCVD and MBE grown samples beyond $N_D > 1 \times 10^{20}$ cm⁻³ as shown in Figure 1b. In consequence, strong mobility decrease was reported limiting the achievable carrier density and specific resistivity. Compensation ratios of the co-sputtered thin films in this work were found to be rather constant up to $N_D = 3.7 \times 10^{20}$ cm⁻³ at higher growth temperatures. A significant increase in compensation ratio (is observed at lower growth temperatures ($\theta = 0.8$), which could be attributed to a decrease in crystal quality where e.g., increasing amount of point defects (e.g., Ga-vacancies). The assumption is consistent with the increase in FWHM and decrease in peak intensity of the second 00.2-reflex observed by XRD. Only reactively sputtered thin films on 2-inch substrates from solid Ga-targets were reported with even higher carrier mobilities in the same range of carrier densities so far. Reported data are even higher than the impurity scattering limit at $\theta = 0$, which was stated to be the result of an underestimation of the effective electron mass but not further discussed. Specific resistivity was derived and compared to reported data from the literature (Figure 2). Lowest specific resistivities in this work were obtained for highest growth temperature (800°C) with $\rho < 0.5$ mΩcm which is close to best reported values in literature independent of the growth method. An increase of resistivity is observed by lowering the growth temperature as a result of the increasing compensation ratio described before. Lowest resistivity of sample A (590°C) was found to be 3.5 mΩcm. The measured carrier concentrations are well beyond the theoretically, required doping to achieve a metallic character. To verify Mott-transition of the sputtered GaN films, temperature-dependent Hall measurements were carried out for $T = 300$ to 575 K. No significant change in electron concentration or electron mobility was observed within the measured temperature range indicating the degenerate nature of the Si-doped GaN films. Temperature-dependent polar optical-phonon scattering was modelled via:

$$\mu_{POP} = \frac{\epsilon_0 \epsilon_r \hbar}{e N m^* F} \sqrt{\frac{\hbar}{2 m^* F \omega_0 (1 + \hbar \omega_0 / E_G)}} \left(1 - 5 \frac{k_B T}{E_G}\right)$$

where $\hbar \omega_0$ is the optical phonon energy (100 meV). Scattering at dislocations is neglected since their impact on transverse mobility above $N_D > 1 \times 10^{20}$ cm⁻³ for dislocation densities below $N_{DISL} < 1 \times 10^{11}$ cm⁻² is not relevant. Dislocation densities of MOCVD-grown GaN on sapphire with AlN nucleation layer (templates used in this work)

are generally found to be lower much lower and the interface of sputtered GaN on MOCVD-GaN is not expected to generate new dislocations. Scattering at grain boundaries could be assumed for sputtered GaN, however, the associated potential barriers would lead to a thermal activation of the carrier mobility or carrier density. In addition, at high doping levels, most of the grain boundary related trap states are filled and the potential barriers would decrease in height and width. Temperature dependent fitting of the carrier mobility was achieved using Equation 2 and 7 by Matthiessens rule given in Figure 2b. Only minor contribution of μ_{POP} was found while μ_{II} clearly dominates the overall low-field scattering in the samples.

In conclusion, heavily doped GaN thin films prepared by co-sputtering from a liquid GaN-target were demonstrated. Extremely high donor concentrations above 3×10^{20} cm⁻³ at low process temperatures (< 800 °C) with specific resistivities below 0.5 mΩcm were achieved. Mott-transition was verified via temperature-dependent Hall-measurements revealing neither a change in mobility nor carrier concentration in the range of 300 to 550 K. Impurity scattering was determined to be the major low-field mobility limiting factor with a minor contribution of polar optical-phonon scattering at elevated temperatures. Scattering at dislocations or grain boundaries was ruled out to impact the total mobility. The results demonstrate the huge potential of sputtering as an alternative route for low-temperature, high throughput and easy upscaling of regrown n-type GaN.

